SIAM J. APPL. MATH.
Vol. 57, No. 2, pp. 327–346, April 1997
© 1997 Society for Industrial and Applied Mathematics
002

ANALYSIS OF A REACTION-DIFFUSION SYSTEM MODELING MAN–ENVIRONMENT–MAN EPIDEMICS*

V. CAPASSO† AND R. E. WILSON‡

Abstract. In this paper an old model for the temporal and spatial evolution of orofecal transmitted disease is reexamined. It consists of a system of two coupled reaction-diffusion equations for the concentration of bacteria and infective humans, under the assumptions that the total population of humans is unaffected by the disease and only a small proportion of the population is affected at any one time. The force of infection on healthy humans is assumed to be a sigmoidal function of bacterial concentration tending to some finite limit, and with zero gradient at zero. (This last feature models an immune response to low concentrations of the infectious agent.) In practice the diffusion coefficient for infective humans is much smaller than that of bacteria and is therefore set to zero; a detailed analysis of the steady-state bifurcation pattern is then performed for the case of homogeneous Dirichlet boundary conditions applied at the endpoints of a one-dimensional interval. Particular attention is paid to the limiting case of small bacterial diffusivity.

A partial analysis of the dynamical behavior of the system, based on monotone techniques, is carried out. It is speculated that the system, subject to homogeneous Dirichlet boundary conditions, has saddle point structure in the natural function space of the problem, similar to the ODE case in which the diffusivity of bacteria is also set to zero. This conjecture is supported by some numerical simulation on both one- and two-dimensional space domains.

Key words. qualitative properties of solutions, reaction-diffusion systems, epidemiology

AMS subject classifications. 35K57, 35Bxx, 92D30

PII. S0036139995284681

1. Introduction.

The spread of infectious diseases due to environmental pollution by an infective human population is one of the main causes of relevant epidemics (cholera, typhoid fever, infectious hepatitis A, malaria, schistosomiasis, etc.) (see, e.g., [2] for extended literature on this subject).

Many results have been obtained for the general theory of man–environment–man epidemics, but the case which has been mostly considered is the one in which there is at most one nontrivial endemic equilibrium: above some parameter threshold a nontrivial state exists, and all epidemic outbreaks tend to it; below the parameter threshold there is no nontrivial state, and all epidemics tend to extinction.

Actually, real data show that a bistable case is more likely to occur, in which the initial condition is relevant. Here (provided we are above some parameter threshold), large outbreaks tend to a nontrivial endemic state which invades the whole habitat; however, small outbreaks tend to extinction and may remain strictly localized in space (see [6], [14]). This may explain why, even though we are exposed to so many infections, only some diseases have evolved into an endemic state.

The mathematical model proposed in [6] and [4] to describe the evolution of fecally-orally transmitted diseases in the coastal regions of the Mediterranean sea (cholera, typhoid fever, infectious hepatitis A) includes, as a basic feature, the positive

*Received by the editors April 17, 1995; accepted for publication (in revised form) January 31, 1996. This research was performed under the auspices of GNFM-CNR (Italy) in the framework of ISS contract n.9203-04.

http://www.siam.org/journals/siap/57-2/28468.html

†Dipartimento di Matematica, Università di Milano, Via Saldini 50, 20133 Milano, Italy (capasso@vmimat.mat.unimi.it).

‡Mathematical Institute, University of Oxford, 24–29 St. Giles, Oxford OX1 3LB, UK (wilson@maths.ox.ac.uk).

feedback interaction between the infective human population and the concentration of the infectious agent in the environment. The human population, once infected, acts as a multiplier of the infectious agent, which is then returned to the environment in fecal excretion; on the other hand, the infectious agent is transmitted to the human population via contaminated food consumption.

If we assume that the total susceptible human population is large with respect to its infective fraction, the basic mathematical model (see [4]) can be written

$$\left.\begin{aligned} \frac{dz_1}{dt}(t) &= -a_{11}z_1(t) + a_{12}z_2(t) \\ \frac{dz_2}{dt}(t) &= -a_{22}z_2(t) + g(z_1(t)) \end{aligned}\right\} \text{ for } t > 0. \tag{1.1}$$

Here $z_1(t)$ denotes the (average) concentration of infectious agent in the environment at time $t \geq 0$; $z_2(t)$ denotes the infective human population at time t; $1/a_{11}$ is the mean lifetime of the agent in the environment; $1/a_{22}$ is the mean infectious period of the human infectives; a_{12} is the multiplicative factor of the infectious agent due to the human population; and finally $g(z_1)$ is the "force of infection" on the human population due to a concentration z_1 of the infectious agent.

The spread of other infectious diseases may be modeled as above, with slight modifications. Schistosomiasis is an important example; see [11].

The choice of g has a strong influence on the dynamical behavior of system (1.1). The case in which g is a monotone increasing function with constant concavity has been analyzed in an extensive way (see [2], [3], [4]); concavity leads to the existence (above a parameter threshold) of exactly one nontrivial endemic state and to its global asymptotic stability.

In [5] and [11] the bistable case (in which system (1.1) has two nontrivial steady states, one of which is a saddle point in the phase plane) was obtained by assuming that the force of infection, as a function of the concentration of the pollutant, is sigma shaped (defined concisely by properties (P1)–(P5) in section 2). In [11] this shape is obtained as a consequence of the sexual reproductive behavior of the schistosomes. In [5] (see also [4]) the case of fecally-orally transmitted diseases was considered; an interpretation of the sigma shape of the force of infection was proposed to model the response of the immune system to environmental pollution: the probability of infection is negligible at low concentrations of the pollutant but increases with larger concentrations; it then becomes concave and saturates to some finite level as the concentration of pollutant increases without limit.

The geographical localization of a small outbreak had never been analyzed before, even though computer simulations in [5] had already shown such a possibility, when the reaction diffusion system modeling the epidemic with spatial structure had been subject to homogeneous Dirichlet boundary conditions. These conditions by themselves are not realistic since they correspond to a completely hostile boundary. On the other hand pure Neumann boundary conditions are also not realistic since they correspond to the complete isolation of the habitat. However, these two extreme cases may provide some insight about the behavior of the system under more general boundary conditions.

In order to consider spatial variations, we study the system

$$\left\{\begin{aligned} u_{1t} &= d\,\Delta u_1 - a_{11}u_1 + a_{12}u_2, \\ u_{2t} &= g(u_1) - a_{22}u_2 \end{aligned}\right. \tag{1.2}$$

for $\mathbf{x} \in \Omega$ (a bounded domain) and $t > 0$, subject to suitable boundary and initial conditions. This system models random dispersal of the pollutant while ignoring the small mobility of the infective human population (see [3]). Here $u_1(\mathbf{x}, t)$ denotes the spatial density of the pollutant at a point $\mathbf{x}$ of the habitat Ω at time $t \geq 0$, and $u_2(\mathbf{x}, t)$ denotes the spatial density of the infective human population.

In [3], [4], existence, uniqueness, and regularity of solutions of the evolution problem related to (1.2), subject to standard linear boundary conditions, were proven. In fact, it was shown that the solution of the initial-boundary value problem associated with system (1.2) is classical for $t \in (0, \infty)$ under suitable regularity assumptions on the data. As a consequence, we shall limit the analysis of the steady states of system (1.2) to classical solutions of the stationary problem

$$\begin{cases} d\,\Delta u_1 - a_{11}u_1 + a_{12}u_2 = 0, \\ g(u_1) - a_{22}u_2 = 0 \end{cases} \tag{1.3}$$

for $x \in \Omega$, subject to suitable boundary conditions.

A rather complete treatment of the qualitative behavior of systems (1.2), (1.3) has been developed in [2], [3], and [4] for the case in which g is a concave function. Concavity of g induces concavity of the evolution operator, which, together with the monotonicity induced by the quasi monotonicity of the reaction terms in (1.2), again imposes uniqueness of the possible nontrivial endemic state.

On the other hand, in the case where g is sigma shaped, monotonicity of the solution operator is preserved, but as we have already observed in the ODE case, uniqueness of nontrivial steady states is no longer guaranteed. Furthermore, the saddle point structure of the phase space cannot be easily transferred from the ODE to the PDE case, as discussed in [5]. (In [5], homogeneous Neumann boundary conditions are analyzed in some detail.) Further, when we have homogeneous Dirichlet boundary conditions or general third-type boundary conditions, nontrivial spatially homogeneous steady states are no longer allowed. For a more extended discussion, the reader is referred to [2] (see also [16]).

In sections 2, 3, and 4 (for the sake of simplicity), we shall refer only to a one-dimensional domain $\Omega = [0, l] \subset \mathbf{R}$, and we shall associate with (1.3) homogeneous Dirichlet boundary conditions.

In section 2 we shall formulate the mathematical problem, introduce ordering of solutions by positive cones, and discuss some general properties of sigmoidal functions.

In section 3 we carry out the steady-state analysis and determine the bifurcation pattern of nontrivial solutions to system (1.3) subject to homogeneous Dirichlet boundary conditions. When the diffusivity of pollutant is small, we show the existence of a narrow bell-shaped steady state, which we conjecture is a saddle point for the dynamics of (1.2). "Small" outbreaks are localized under this bell-shaped steady state.

In section 4, we use monotone methods to carry out a partial analytical study of the evolution problem. The conjectured saddle point structure and stability of nontrivial steady states have been supported by computer simulation. We leave the complete rigorous stability analysis to a subsequent paper.

In section 5, we consider multidimensional space domains Ω, again with homogeneous Dirichlet boundary conditions in force. (We will mainly concentrate on two-dimensional examples.) We present numerical simulations which seem to confirm that, here also, provided that Ω is convex, (1.2) inherits the bistable structure of the underlying ODE system (1.1).

2. The mathematical problem. Notation and preliminary analysis. The aim of this paper is to study the system of a linear parabolic equation coupled with an ODE defined by

$$\left\{\begin{array}{lcl} \dfrac{\partial}{\partial t}u_1(x,t) &=& d\,\dfrac{\partial^2}{\partial x^2}u_1(x,t) - a_{11}u_1(x,t) + a_{12}u_2(x,t), \\ \dfrac{\partial}{\partial t}u_2(x,t) &=& -a_{22}u_2(x,t) + a_{21}g(u_1(x,t)) \end{array}\right. \tag{2.1}$$

for $x \in (0,l)$, $t > 0$, subject to the boundary conditions

$$u_1(0,t) = u_1(l,t) = 0 \qquad \text{for } t > 0. \tag{2.2}$$

System (2.1), (2.2) is supplemented by the initial conditions

$$u_1(x,0) = u_1^0(x), \qquad u_2(x,0) = u_2^0(x) \qquad \text{for } x \in (0,l), \tag{2.3}$$

not both identically zero. We let $\mathbf{u}(t)$ denote $(u_1(\cdot,t), u_2(\cdot,t))$, a member of a suitable function space.

We shall assume that d, a_{11}, a_{12}, a_{21}, and a_{22} are positive real constants and that the function $g : \mathbf{R}_+ \to \mathbf{R}_+$ satisfies the following properties:

(P1) $g \in C^2(\mathbf{R}_+)$;
(P2) $g(0) = g'(0) = 0$;
(P3) $g'(z) > 0$ for any $z > 0$;
(P4) $\lim_{z\to\infty} g(z) = 1$;
(P5) $\exists\, \xi > 0$ such that $g''(z) > 0$ for $z \in (0,\xi)$ and $g''(z) < 0$ for $z \in (\xi,\infty)$.

We may rescale problem (2.1)–(2.3) by putting $x = l\tilde{x}$, $t = \tilde{t}/a_{11}$, $d = a_{11}l^2\tilde{d}$, and $v = a_{21}\tilde{v}/a_{11}$ so that on removal of tildes we have

$$\left\{\begin{array}{lcl} \dfrac{\partial u_1}{\partial t}(x,t) &=& d\,\dfrac{\partial^2 u_1}{\partial x^2}(x,t) - u_1(x,t) + \alpha u_2(x,t), \\ \dfrac{\partial u_2}{\partial t}(x,t) &=& -\beta u_2(x,t) + g(u_1(x,t)) \end{array}\right. \tag{2.4}$$

for $x \in (0,1)$ and $t > 0$. Here $\alpha = a_{12}a_{21}/a_{11}^2$ and $\beta = a_{22}/a_{11}$. In the following discussion we shall use

$$\gamma := \frac{\alpha}{\beta} = \frac{a_{12}a_{21}}{a_{11}a_{22}}$$

as one of the bifurcation parameters; with reference to system (1.2) it may be interpreted as "global" information about the positive feedback strength of the coupling between the human population and the environmental pollution (scaled by the natural rate of decay of the pollutant and the infectious period of an infected individual).

During our treatment we shall also refer to the associated ODE system

$$\left\{\begin{array}{lcl} \dfrac{dz_1}{dt}(t) &=& -z_1(t) + \alpha\, z_2(t), \\ \dfrac{dz_2}{dt}(t) &=& -\beta\, z_2(t) + g(z_1(t)) \end{array}\right. \tag{2.5}$$

for $t > 0$. We define $\mathbf{z}(t) := (z_1(t), z_2(t)) \in \mathbf{R}^2$.

Because of the assumptions made on g, system (2.5) is a quasi-monotone (increasing) system (see [2, pp. 230ff]. This term means that dz_i/dt is nondecreasing in z_j for $i \neq j$.); this implies that (2.4) is a quasi-monotone reaction-diffusion system.

Under the above assumptions, it can be shown (see [3]) that a unique solution exists for problem (2.4),(2.2) for any sufficiently regular initial condition (2.3). Moreover, due to the assumptions made on g, any solution may be extended to all $t \in [0, \infty)$. Furthermore, under sufficient regularity assumptions on the data, it may be shown that solutions are classical solutions; that is,

$$u_1 \in C^{2,1}(\Omega \times (0, +\infty); \mathbf{R}) \cap C^{1,0}(\overline{\Omega} \times (0, +\infty); \mathbf{R}),$$
$$u_2 \in C^{0,1}(\overline{\Omega} \times (0, +\infty); \mathbf{R}).$$

We may then carry out our analysis in the Banach space $X := C(\overline{\Omega}; \mathbf{R}^2) \ni \mathbf{u}(t)$ with norm $\|\mathbf{u}\| = \|(u_1, u_2)\| = \sup_{x\in\overline{\Omega}} |u_1(x)| + \sup_{x\in\overline{\Omega}} |u_2(x)|$. X is an ordered Banach space with partial order induced by the cone

$$X_+ := \left\{\mathbf{u} = (u_1, u_2) \in X : \, u_1(x) \geq 0, \, u_2(x) \geq 0, \, x \in \overline{\Omega}\right\}.$$

We shall say $\mathbf{u}^* \leq \mathbf{u}^{**}$ if $\mathbf{u}^{**} - \mathbf{u}^* \in X_+$; $\mathbf{u}^* < \mathbf{u}^{**}$ shall mean that $\mathbf{u}^* \leq \mathbf{u}^{**}$ and that $\mathbf{u}^* \neq \mathbf{u}^{**}$; $\mathbf{u}^* \ll \mathbf{u}^{**}$ shall mean that $u_1^{**}(x) - u_1^*(x) > 0$ and $u_2^{**}(x) - u_2^*(x) > 0$ for all $x \in \Omega$. If $\mathbf{u}^* \leq \mathbf{u}^{**}$, we may introduce the order interval

$$[\mathbf{u}^*, \mathbf{u}^{**}] = \left\{\mathbf{u} = (u_1, u_2) \in X : \begin{array}{l} u_1^*(x) \leq u_1(x) \leq u_1^{**}(x), \\ u_2^*(x) \leq u_2(x) \leq u_2^{**}(x), \end{array} \, x \in \overline{\Omega}\right\}.$$

(Similar notation may be adopted for comparison in $\mathbf{R}^2$ of solutions $\mathbf{z}$ to ODE system (2.5).)

For any sufficiently smooth initial condition $\mathbf{u}_0 \in X_+$, we may obtain a unique global solution $\{\mathbf{u}(t), t \in \mathbf{R}_+\}$. This identifies an evolution operator $\{\mathcal{U}(t), t \in \mathbf{R}_+\}$ on X_+ which satisfies the following properties:

(1) $\mathcal{U}(0) = I$.

(2) $\mathcal{U}(t)\mathcal{U}(s) = \mathcal{U}(t + s)$ for $s, t \in \mathbf{R}_+$.

(3) $\mathcal{U}(t)\mathbf{0} = \mathbf{0}, \; t \in \mathbf{R}_+$.

(4) For any $t \geq 0$, the map $\mathbf{u}_0 \in X_+ \mapsto \mathcal{U}(t)\mathbf{u}_0 \in X$ is continuous, uniformly for $t \in [t_1, t_2] \subset \mathbf{R}_+$.

(5) For any $\mathbf{u}_0 \in X_+$, the map $t \in \mathbf{R}_+ \mapsto \mathcal{U}(t)\mathbf{u}_0$ is continuous.

Due to the quasi monotonicity of system (1.2), we may use comparison theorems (see [2]) to state that

(6) $\mathbf{u}_0, \overline{\mathbf{u}}_0 \in X_+, \, \mathbf{u}_0 \leq \overline{\mathbf{u}}_0 \Rightarrow \mathcal{U}(t)\mathbf{u}_0 \leq \mathcal{U}(t)\overline{\mathbf{u}}_0, \, t > 0$.

These properties imply the strong properties of $\mathcal{U}(t)$:

(7) $\mathbf{u}_0 \in X_+ \Rightarrow \mathcal{U}(t)\mathbf{u}_0 \in X_+, \, t \in \mathbf{R}_+$.

(8) $\mathbf{u}_0 \in X_+, \mathbf{u}_0 \neq \mathbf{0} \Rightarrow \mathcal{U}(t)\mathbf{u}_0 \gg \mathbf{0}, \, t > 0$.

(9) $\mathbf{u}_0, \overline{\mathbf{u}}_0 \in X_+, \, \mathbf{u}_0 \leq \overline{\mathbf{u}}_0, \, \mathbf{u}_0 \neq \overline{\mathbf{u}}_0, \Rightarrow \mathcal{U}(t)\mathbf{u}_0 \ll \mathcal{U}(t)\overline{\mathbf{u}}_0, \, t > 0$.

Thanks to the quasi-monotone structure of the ODE system (2.5), its qualitative behavior has been described in detail. In particular the following results are known (see [2] and [5]).

PROPOSITION 2.1. *There exists a $\gamma_{crit} > 0$ such that*

(i) *For $\gamma < \gamma_{crit}$, the trivial solution $(0, 0) \in \mathbf{R}^2$ is the only equilibrium for ODE system* (2.5). *It is globally asymptotically stable (GAS) in the positive cone* $\mathbf{K}$ *of* $\mathbf{R}^2$.

(ii) *For $\gamma = \gamma_{crit}$, system* (2.5) *admits a unique nontrivial equilibrium in addition to* $(0, 0)$.

(iii) *For $\gamma > \gamma_{crit}$, system* (2.5) *admits three equilibria in the positive cone* $\mathbf{K}$*; the trivial one* $\mathbf{0} = (0,0)$ *and two other nontrivial equilibria* $\mathbf{z}^-$ *and* $\mathbf{z}^+$ *such that*

$$\mathbf{0} \ll \mathbf{z}^- \ll \mathbf{z}^+.$$

In this case $\mathbf{z}^-$ *is a saddle point; the stable manifold* M_+ *of* $\mathbf{z}^-$ *is the separatrix of the domain of attraction dom*$(\mathbf{0})$ *of the trivial solution and the domain of attraction dom*$(\mathbf{z}^+)$ *of* $\mathbf{z}^+$:

$$\mathbf{K} = M_+ \cup \mathrm{dom}(\mathbf{0}) \cup \mathrm{dom}(\mathbf{z}^+),$$

and these sets are disjoint subsets of $\mathbf{K}$. $\mathbf{0}$ *and* $\mathbf{z}^+$ *are GAS in their own domains of attraction.*

Proposition 2.1 may be proven from the following argument. Let g be a sigmoidal function satisfying properties (P1)–(P5) above. Let $\gamma > 0$, and define $f_\gamma : [0,\infty) \to \mathbf{R}$ by

$$f_\gamma(z) = z - \gamma g(z).$$

The equilibria of system (2.5) then correspond to the zeroes of f_γ in $[0,+\infty)$. (Clearly $f_\gamma(0) = 0$.) It is then geometrically clear (recalling the properties of sigmoidal functions) that there exists a critical value $\gamma_{crit} > 0$ such that

(i) for $\gamma < \gamma_{crit}$, $f_\gamma(z) > 0$ for any $z > 0$.

(ii) for $\gamma = \gamma_{crit}$, $f_\gamma(z) \geq 0$ and there exists a unique $z^c > 0$ such that $f_\gamma(z^c) = 0$ and $f'_\gamma(z^c) = 0$.

(iii) for $\gamma > \gamma_{crit}$, f_γ admits exactly two distinct zeroes z^- and z^+ such that $0 < z^- < z^+$, $f'_\gamma(z^-) < 0$, and $f'_\gamma(z^+) > 0$ so that $f_\gamma(z) > 0$ for $0 < z < z^-, z > z^+$, and $f_\gamma(z) < 0$ for $z^- < z < z^+$. As functions of γ, z^-, and z^+ are continuous and moreover are (strictly) monotone decreasing and monotone increasing, respectively. Simple analytical proofs of these statements appear in [17].

Later, we shall also need to know properties of the function $F_\gamma : [0,+\infty) \to \mathbf{R}$ defined by

$$F_\gamma(z) := \int_0^z f_\gamma(s)ds,$$

for $z \geq 0$. If we let $\mathcal{F} : \gamma \in [\gamma_{crit}, +\infty) \mapsto \mathcal{F}(\gamma) := F_\gamma(z^+(\gamma)) \in \mathbf{R}$, then the following proposition holds.

LEMMA 2.2. (i) $\mathcal{F}$ *is a continuous, strictly monotone decreasing function,* (ii) $\mathcal{F}(\gamma_{crit}) > 0$, *and* (iii) $\lim_{\gamma\to+\infty} \mathcal{F}(\gamma) = -\infty$.

Sketch of proof. (i) Continuity is clear. Now $\mathcal{F}(\gamma) = \int_0^{z^+(\gamma)} f_\gamma(s)ds$. Partition the range of integration, putting $I_1 = \int_0^{z^-(\gamma)} f_\gamma(s)ds$ and $I_2 = -\int_{z^-(\gamma)}^{z^+(\gamma)} f_\gamma(s)ds$ so that I_1, I_2 are positive and $\mathcal{F}(\gamma) = I_1 - I_2$. Now z^- and z^+ are, respectively, monotone decreasing (to 0) and monotone increasing; thus the range of integration of I_1 decreases monotonically (in length to 0), whereas that of I_2 is monotone increasing; moreover, for s fixed in the range of I_1, $f_\gamma(s)$ is monotone decreasing with γ. Similarly for s fixed in the range of I_2, $-f_\gamma(s)$ is monotone increasing with γ. Hence I_1 is monotone decreasing, and I_2 is monotone increasing with respect to γ. Hence $\mathcal{F}(\gamma)$ is monotone decreasing. (ii) For $\gamma = \gamma_{crit}$, $f_\gamma(s) > 0$ for $s > 0$, $\neq z^c$. So $\int_0^{z^c} f_\gamma(s)ds > 0$. (iii) It is easy to show that $I_1 \downarrow 0$ as $\gamma \to \infty$. By constructing triangles under $-f_\gamma(s)$, $s \in (z^-, z^+)$, it is possible to show that $I_2 \uparrow \infty$. For full details, see [17]. □

As a consequence of Lemma 2.2, $\mathcal{F}$ must have a unique zero at $\gamma_D > \gamma_{crit}$. Thus (i) $\mathcal{F}(\gamma) > 0$ for $\gamma_{crit} \leq \gamma < \gamma_D$, (ii) $\mathcal{F}(\gamma_D) = 0$, (iii) $\mathcal{F}(\gamma) < 0$ for $\gamma > \gamma_D$.

3. Steady-state analysis. As announced earlier, we wish to analyze the steady states of system (2.1) subject to homogeneous Dirichlet boundary conditions. Hence we are looking for the classical solutions of the semilinear elliptic problem

$$\left\{ \begin{array}{rcl} d\,u_1''(x) - u_1(x) + \alpha u_2(x) & = & 0, \\ g(u_1(x)) - \beta u_2(x) & = & 0 \end{array} \right. \tag{3.1}$$

for $x \in (0,1)$, subject to homogeneous Dirichlet boundary conditions.

Using the notation introduced in section 2, we may reduce (3.1) to the equivalent equation

$$d\,u_1''(x) - f_\gamma(u_1(x)) = 0, \qquad x \in (0,1). \tag{3.2}$$

By ignoring boundary conditions (for the present), (3.2) is equivalent to the ODE system

$$\left\{ \begin{array}{rcl} u'(x) & = & v(x), \\ v'(x) & = & f_\gamma(u(x))/d \end{array} \right. \tag{3.3}$$

for $x \in \mathbf{R}$.

We look for the general integral of (3.3), and later we shall select those solutions which satisfy the required boundary conditions; system (3.3) is a classical Hamiltonian system with total energy (see [1, pp. 79ff])

$$H(u,v) := \frac{v^2}{2} - \frac{1}{d}F_\gamma(u), \qquad (u,v) \in \mathbf{R}^2. \tag{3.4}$$

So the orbits in the (u,v) phase plane must lie on the level curves of the total energy $H(u,v) = \text{const}$. That is, the general integral of (3.3) is given by

$$\frac{v^2}{2} - \frac{1}{d}F_\gamma(u) = c/d, \qquad c \in \mathbf{R}, \tag{3.5}$$

or in explicit form

$$v = \pm\sqrt{\frac{2}{d}}\sqrt{F_\gamma(u) + c}, \qquad c \in \mathbf{R}. \tag{3.6}$$

The topology of the phase plane is now determined in the standard way [1, section 12] by a comparison of $F_\gamma(u)$ at $u = 0$ and at $z^+(\gamma)$, where it takes local minimum values 0 and $\mathcal{F}(\gamma)$, respectively, so that both $(0,0)$ and $(0, z^+(\gamma))$ are saddle points. On the other hand, $F_\gamma(u)$ has a local minimum at $z^-(\gamma)$ so that there is a center at $(z^-(\gamma), 0)$ (see [7] and [1, section 12]).

We mentioned that for $\gamma \le \gamma_{crit}$ system (3.1) may not have nontrivial equilibria when subject to homogeneous Dirichlet boundary conditions (see [5]). In fact, it was proven in [5] (also [10]) that for

$$\gamma < \gamma_{crit}(1 + d\lambda_1),$$

the equilibrium $\mathbf{0}$ is GAS in the positive cone X_+, where $\lambda_1 > 0$ is the first eigenvalue of the elliptic problem

$$\left\{ \begin{array}{l} \Delta\phi + \lambda\phi = 0, \\ \phi(0) = \phi(1) = 0. \end{array} \right. \tag{3.7}$$

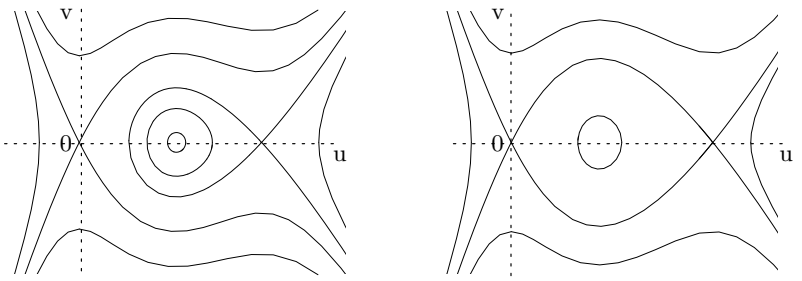

(a) (b)

FIG. 3.1. (u, v) *phase plane topologies for* (a) $\gamma_{crit} < \gamma < \gamma_D$ *and for* (b) $\gamma = \gamma_D$.

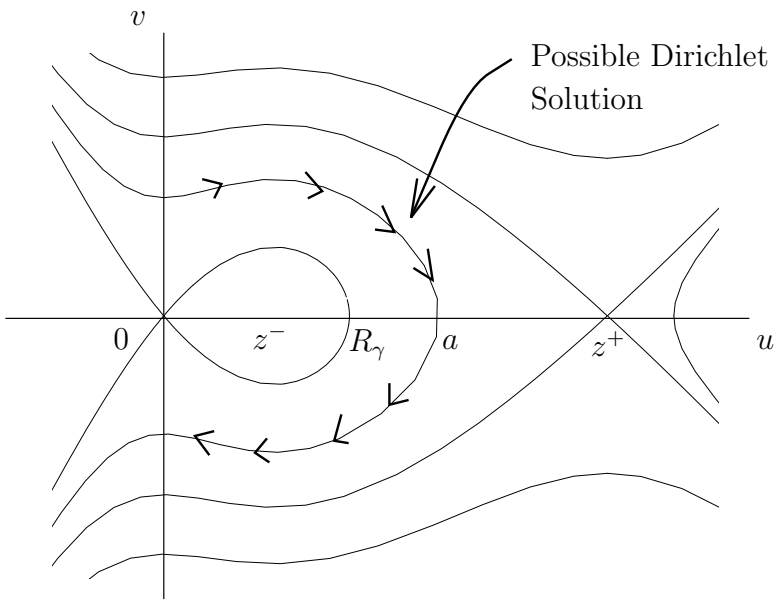

FIG. 3.2. *Phase plane topology for* $\gamma > \gamma_D$.

Now (i) for $\gamma \in (\gamma_{crit}, \gamma_D)$, we have $\mathcal{F}(\gamma) > 0$, so $u = 0$ is the unique global minimum of $F_\gamma(u)$. (ii) We have $\mathcal{F}(\gamma_D) = 0$ so that for $\gamma = \gamma_D$, $F_\gamma(u)$ has two equal local minima at 0 and $u_+(\gamma)$. (iii) For $\gamma > \gamma_D$, we have $\mathcal{F}(\gamma) < 0$ so that $F_\gamma(u)$ has a unique global minimum at $u_+(\gamma)$. Figures 3.1(a), 3.1(b), and 3.2 show the phase plane topologies for these three cases.

It is now clear that the only case which allows solutions of (3.2) satisfying homogeneous Dirichlet boundary conditions is $\gamma > \gamma_D$ (see Figure 3.2).

In fact, these solutions correspond to phase plane trajectory segments which start and end on the v axis such that the change in x as the segment is traversed is equal to the length of the space interval, in our case unity; see [8, p. 7] and [16]. If the upper trajectory segment under consideration is $\mathcal{C}$, we therefore require, using symmetry

(and noting $v \to 0$ at the endpoint) that

$$\begin{aligned}\frac{1}{2} &= \int_{\mathcal{C}} dx, \\ &= \int_{\mathcal{C}} \left(\frac{du}{dx}\right)^{-1} \left(\frac{du}{dx}\right) dx, \\ &= \int_{\mathcal{C}} \frac{du}{v}.\end{aligned}$$

(See [16].) If we let a be the intersection of $\mathcal{C}$ with the u-axis (see Figure 3.2), we therefore require

$$\frac{1}{2} = \int_0^a \frac{\sqrt{d/2}}{\sqrt{F_\gamma(u) - F_\gamma(a)}} du,$$

using formula (3.6) for phase plane trajectories. We must take $a \in (R_\gamma, z^+(\gamma))$, where R_γ is the least positive zero of F_γ, so that $(R_\gamma, 0)$ is the point of intersection of the homoclinic separatrix attached to $(0,0)$ with the u-axis (again see Figure 3.2).
For analytical convenience we define

$$I(a) = \int_0^a \frac{du}{\sqrt{F_\gamma(u) - F_\gamma(a)}}$$

so that homogeneous Dirichlet solutions correspond to intersections of $I(a)$ with the level $1/\sqrt{2d}$. The bifurcation problem for Dirichlet solutions may now be reduced to studying $I(a)$ for $a \in (R_\gamma, z^+(\gamma))$. It can be shown easily that I has singularities at R_γ and $z^+(\gamma)$, with $I(a) \uparrow \infty$ as $a \downarrow R_\gamma$ or as $a \uparrow z^+(\gamma)$. Moreover, I is C^1 smooth and positive for $a \in (R_\gamma, z^+(\gamma))$. By simple continuity arguments, I must therefore attain a global minimum of value M_γ, say, at some $a^* \in (R_\gamma, z^+(\gamma))$.

We may now use d as a second bifurcation parameter and recognize that (i) for $d > 1/2M_\gamma^2$, we may not have nontrivial solutions; (ii) for $d < 1/2M_\gamma^2$, there are at least two nontrivial solutions; and (iii) for $d = 1/2M_\gamma^2$, the number of nontrivial solutions is equal to the number of times I attains its global minimum M_γ.

Similar conclusions were reached in [10] by using a more sophisticated variational technique. However, the qualitative methods used there do not give information on the exact number, or structure, of solutions.

The following lemma guarantees that we have at most two nontrivial solutions to the homogeneous Dirichlet problem.

LEMMA 3.1. *$I(a)$ is continuously differentiable and has at most one local minimum in $(R_\gamma, z^+(\gamma))$.*

Sketch of proof. This is a small extension of Theorem 2.1 in [16]. There, the corresponding result is proved for cubic f. In our case we may use the mean value theorem to deduce the existence of $\tilde{a}$ such that $I'(a) < 0$ for $a \in (R_\gamma, \tilde{a})$, and $I''(a) + 3I'(a)/a > 0$ for $a \in (\tilde{a}, z^+(\gamma))$. (This last result is derived in [16] with explicit computation on the polynomial coefficients.) It follows that I has at most one local minimum (since otherwise there is at least one local maximum which contradicts the inequality above) at $a^* \in (\tilde{a}, z^+(\gamma))$. A complete proof of this lemma appears in [17]. □

In addition, we have the following result.

LEMMA 3.2. *M_γ is a decreasing function of γ.*

Proof. Recall that $z^+(\gamma)$ is increasing with γ. Moreover, R_γ is decreasing with γ. (Proof: R_γ is the least positive zero of $F_\gamma(u) = \int_0^u (s - \gamma g(s)) ds$. So for $\gamma_2 > \gamma_1$,

$F_{\gamma_2} < F_{\gamma_1}$. Hence $F_{\gamma_2}(R_{\gamma_1}) < 0$, so by the intermediate value theorem, $R_{\gamma_2} < R_{\gamma_1}$.) We have

$$I_\gamma(a) = a \int_0^1 (\Delta F_\gamma)^{-1/2}\, d\tilde{u},$$

where

$$\Delta F_\gamma = \int_{a\tilde{u}}^{a} (\gamma g(s) - s)\, ds$$

for $\tilde{u} \in (0,1)$. For fixed $\tilde{u}$, $\Delta F_{\gamma_2} > \Delta F_{\gamma_1}$, so $(\Delta F_{\gamma_2})^{-1/2} < (\Delta F_{\gamma_1})^{-1/2}$, and hence $I_{\gamma_2}(a) < I_{\gamma_1}(a)$ for $a \in D(I_{\gamma_1})$. But $D(I_{\gamma_2}) \supset D(I_{\gamma_1})$, and so $M_{\gamma_2} = \min I_{\gamma_2} < \min I_{\gamma_1} = M_{\gamma_1}$ as claimed. □

We may now identify

$$d_{crit} := \frac{1}{2\, M_\gamma^2} > 0$$

such that the following bifurcation theorem holds.

THEOREM 3.3. *Consider the system* (3.1) *subject to homogeneous Dirichlet boundary conditions.*

(1) *If* $0 \le \gamma \le \gamma_D$, *then the system admits only the trivial solution* $u_1(x) = u_2(x) = 0$, *for* $x \in [0,1]$.
(2) *If* $\gamma > \gamma_D$, *then a critical value* $d_{crit}(\gamma)$ *exists such that*
   (a) *for* $d > d_{crit}(\gamma)$, $\mathbf{u} = \mathbf{0}$ *is the only solution;*
   (b) *for* $d = d_{crit}(\gamma)$, *there is exactly one nontrivial solution* $\mathbf{u}^c$ *such that* $(u_1^c(x), u_2^c(x)) \gg \mathbf{0}$;
   (c) *for* $d < d_{crit}(\gamma)$, *there are exactly two nontrivial solutions* $\mathbf{u}^- = (u_1^-(x), u_2^-(x))$ *and* $\mathbf{u}^+ = (u_1^+(x), u_2^+(x))$ *such that* $\mathbf{0} \ll \mathbf{u}^- \ll \mathbf{u}^+$.

Because of Lemma 3.2, $d_{crit} = 1/2M_\gamma^2$ is increasing with γ so that as γ is increased, we do not require diffusion to be as small for the existence of nontrivial solutions to (3.1).

Theorem 3.3 is a two-parameter threshold result, requiring both $\gamma > \gamma_D$ and $d > d_{crit}$ for existence of solutions. Because d_{crit} depends on γ in a complicated way, it is difficult to identify a single threshold parameter.

Now suppose that $\gamma > \gamma_D$, and $d < d_{crit}(\gamma)$ (Theorem 3.3, case 2(c)) so that the problem (3.1) with homogeneous Dirichlet boundary conditions admits exactly two nontrivial solutions, $\mathbf{u}^-$ and $\mathbf{u}^+$. If a^- and a^+ denote the amplitudes ($\max |u_1^\pm|$) of $u_1^-(x)$ and $u_1^+(x)$, respectively, then we have

$$R_\gamma < a^- < a^+ < z^+(\gamma).$$

Also, by simple comparison arguments, $u_1^-(x) < u_1^+(x)$ for all $x \in (0,1)$; consequently $u_2^-(x) < u_2^+(x)$ for all $x \in (0,1)$, since the second equation of system (3.1) is monotone. Hence $\mathbf{u}^- \ll \mathbf{u}^+$, as claimed in Theorem 3.3.

We may say more concerning the structure of $\mathbf{u}^-$ and $\mathbf{u}^+$. First note that $\mathbf{u}^-$ and $\mathbf{u}^+$ are symmetric about $x = 1/2$ by the $v \mapsto -v$ symmetry in the phase plane. Now, in the singular limit $d \downarrow 0$, we require $I(a^-)$, $I(a^+) \uparrow \infty$. It can then be shown that $a^- \downarrow R_\gamma$ and $a^+ \uparrow z^+(\gamma)$. In this way, the phase plane trajectory segment $(u_1^-, u_1^{-\prime})$ approaches the homoclinic orbit attached to $(0,0)$; that for $(u_1^+, u_1^{+\prime})$ approaches the heteroclinic separatrices attached to $(z^+(\gamma), 0)$.

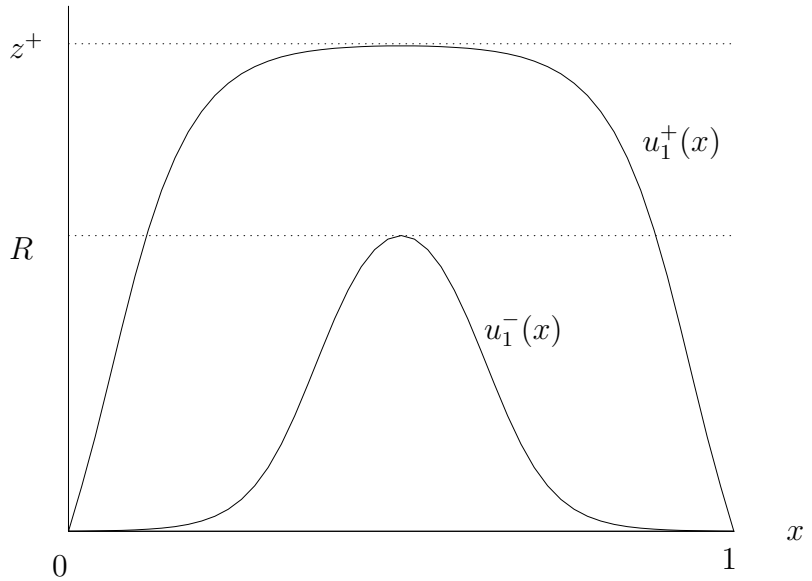

FIG. 3.3. *Shooting method computations of the steady states* $u_1^-(x)$ *and* $u_1^+(x)$*, with* $g(u) = u^2/(1+u^2)$*,* $\gamma = 2.3 > \gamma_D \simeq 2.17$*,* $d = 0.0025 < d_{crit}$*. To four decimal places,* $a^+ = 1.7105$*,* $z^+ = 1.7179$*,* $a^- = 1.0420$*,* $R = 1.0420$ *(but note* $a^- > R$*).*

In the first case, the largest contribution to the time map comes from the neighborhood of the equilibrium point $(0,0)$ so that $u_1^-(x), u_1^{-\prime}(x) \simeq 0$ through most of $(0,1)$. There is a "fast" trip around the homoclinic loop; this corresponds to a "hump" of width $O(\sqrt{d})$ centered at $x = 1/2$, whose height is bounded below by R_γ, no matter how small d.

In the second case, the most significant contribution to the time map comes from the neighborhood of $(z^+(\gamma), 0)$ so that $u_1^+(x) \simeq z^+(\gamma)$, $u_1^{+\prime}(x) \simeq 0$ throughout most of the domain. There are boundary layers of width $O(\sqrt{d})$ connecting the solution to the homogeneous Dirichlet data at $x = 0, 1$.

In Figure 3.3, some sample plots of $u_1^-(x)$ and $u_1^+(x)$ are given. The infective human concentrations, u_2^- and u_2^+, have structure similar to that of their bacterial counterparts.

4. The evolution problem. We again suppose that $\gamma > \gamma_D$ and that $d < d_{crit}(\gamma)$ so that the conclusions of Theorem 3.3, case 2(c), hold.

Due to the monotonicity properties of the evolution operator $\{\mathcal{U}(t),\, t \in \mathbf{R}_+\}$ of system (2.1), we may claim that if $\mathbf{u}(t)$ is a solution to system (2.1) with initial data $\mathbf{u}_0$, then (i) $\mathbf{0} \le \mathbf{u}_0 \le \mathbf{u}^-$ implies that $\mathbf{0} \le \mathbf{u}(t) \le \mathbf{u}^-$ for all $t \ge 0$; on the other hand, (ii) $\mathbf{u}^- \le \mathbf{u}_0 \le \mathbf{u}^+$ implies that $\mathbf{u}^- \le \mathbf{u}(t) \le \mathbf{u}^+$ for all $t \ge 0$. In this way solutions whose initial data are "sandwiched" by a pair of steady states remain "sandwiched" for all time. We also know from [5] that $(0,0)$ is locally asymptotically stable.

As an extension of Proposition 2.1 we conjecture that $\mathbf{u}^- = (u_1^-(x), u_2^-(x))$, $x \in (0,1)$, is a saddle point for system (3.1), while $\mathbf{0}$ and $\mathbf{u}^+ = (u_1^+(x), u_2^+(x))$, $x \in (0,1)$, are stable attractors. To this end, let us observe the following.

LEMMA 4.1. *Under the assumptions of Theorem* 3.3*, case* 2(c)*, the system*

$$\left\{ \begin{array}{rcl} d\, w_1''(x) - w_1(x) + (\alpha - \epsilon) w_2(x) & = & 0, \\ g(w_1(x)) - \beta w_2(x) & = & 0 \end{array} \right. \tag{4.1}$$

for $x \in \Omega$ and subject to homogeneous Dirichlet boundary conditions admits two nontrivial classical solutions for a suitable choice of $\epsilon > 0$. Each of them is a lower solution of problem (3.1).

Proof. We may just observe that for sufficiently small $\epsilon > 0$ the continuity of γ_D and d_{crit} with respect to γ confirms the results of Theorem 3.3. Now take any nontrivial solution (w_1, w_2) of (4.1). We have

$$d\, w_1''(x) - w_1(x) + \alpha w_2(x) = \epsilon w_2(x) \geq 0,$$
$$g(w_1(x)) - \beta w_2(x) = 0,$$

which shows that $(w_1(x), w_2(x))$ is a lower solution of problem (3.1). □

LEMMA 4.2. *Under the assumptions of Theorem* 3.3*, case* 2(c)*, the system*

$$\begin{cases} -z_1 + \alpha z_2 & = & 0, \\ -\beta z_2 + g(z_1) & = & 0 \end{cases} \tag{4.2}$$

admits two nontrivial solutions. Each of them is a spatially homogeneous upper solution for system (3.1) *subject to homogeneous Dirichlet boundary conditions.*

Proof. We need only observe that $z_1 \geq 0$ and $z_2 \geq 0$ at the boundary. □

Let us denote by $\underline{\mathbf{u}} = \{(\underline{u}_1(x), \underline{u}_2(x)),\, x \in \Omega\}$ the smallest of the nontrivial solutions of problem (4.1) and by $\overline{\mathbf{u}} = \{(\overline{u}_1(x), \overline{u}_2(x)),\, x \in \Omega\}$ the largest of the nontrivial solutions of problem (4.2).

By use of comparison theorems we may claim that the largest nontrivial solution $\mathbf{u}^+$ of system (3.1) satisfies

$$\underline{\mathbf{u}} \leq \mathbf{u}^+ \leq \overline{\mathbf{u}}.$$

Further, we may claim that $\mathcal{U}(t)\underline{\mathbf{u}}$ is monotone nondecreasing in $t \in \mathbf{R}_+$, while $\mathcal{U}(t)\overline{\mathbf{u}}$ is monotone nonincreasing in $t \in \mathbf{R}_+$, and by further use of comparison theorems

$$\mathcal{U}(t)\underline{\mathbf{u}} \leq \mathbf{u}^+ \leq \mathcal{U}(t)\overline{\mathbf{u}},$$

for $t \geq 0$. We have thus built a *contracting rectangle* containing the equilibrium point $\mathbf{u}^+$ in the function space X.

Unfortunately we cannot apply the convergence theorem of contracting rectangles in Banach spaces [2] because the evolution operator $\mathcal{U}(t)$ is not compact. This is because the second equation in system (3.1) is an ODE. We leave further discussion about this point to a subsequent paper.

We now give some computer simulations which seem to indicate that the contracting rectangle does indeed converge to the nontrivial equilibrium $\mathbf{u}^+$, thus showing global asymptotic stability of this point in the rectangle $[\underline{\mathbf{u}}, \overline{\mathbf{u}}]$ of X_+.

EXPERIMENT 1. *As with all our numerical simulations, we took $g(u) = u^2/(1 + u^2)$. (One advantage of this choice is that we may easily integrate to find $F_\gamma(u) = u^2/2 - \gamma u + \gamma \tan^{-1} u$.) We took $\alpha = 2.3$ and $\beta = 1$ so that $\gamma = 2.3 > \gamma_D \simeq 2.1750629627$. We took $d = 0.0025 < d_{crit}$. Under these conditions, the steady states $u_1^-(x)$ and $u_1^+(x)$ were found by a shooting method ($u_2^-(x)$ and $u_2^+(x)$ are then easily determined); these steady states are plotted in Figure* 3.3*. For our first experiment we took initial data*

$$u_1^0(x) = u_1^-(x) + x(1 - x)/10,$$
$$u_2^0(x) = g(u_1^0(x)).$$

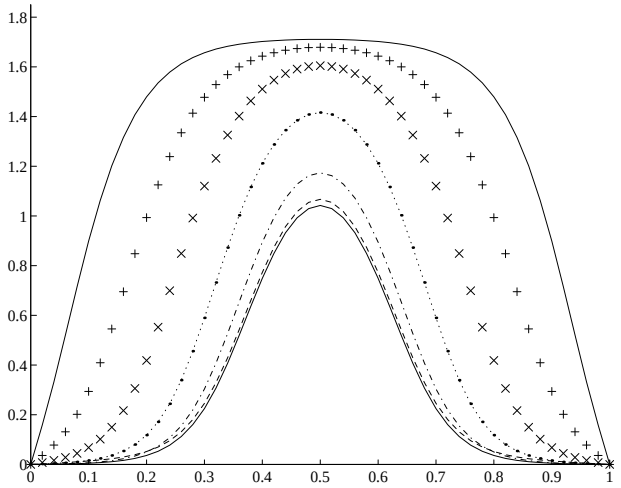

FIG. 4.1. *Results of Experiment* 1, u_1 *against* x, *with steady states* u_1^- *and* u_1^+. *Steady states,* –; $t = 0$, - -; $t = 20$, -.; $t = 40$, ..; $t = 60$, ×; $t = 80$, +.

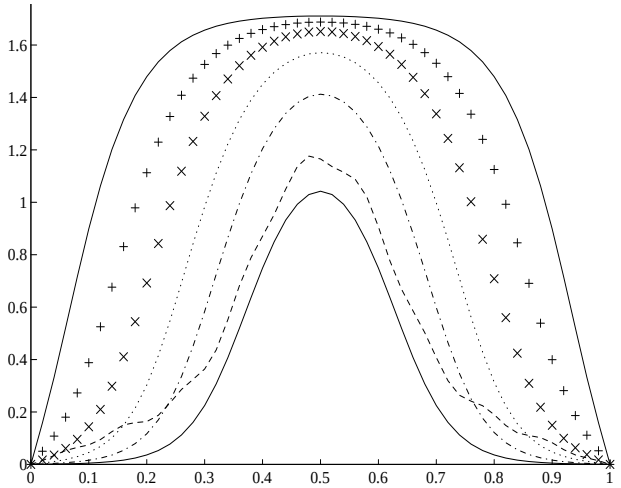

FIG. 4.2. *Results of Experiment* 2, u_1 *against* x, *with steady states* u_1^- *and* u_1^+. *Steady states,* –; $t = 0$, - -; $t = 15$, -.; $t = 30$, ..; $t = 45$, ×; $t = 60$, +.

Note that $\mathbf{u}_0$, $= (u_1^0, u_2^0) \in [\mathbf{u}^-, \mathbf{u}^+]$. *The evolution of* u_1 *is depicted in Figure* 4.1. *The evolution of* u_2 *took a similar course and is not shown. Certainly, it seems that this choice of initial data is attracted to* $\mathbf{u}^+$.

EXPERIMENT 2. *We took the same parameter choices as in Experiment* 1. *However, we chose the more complicated initial data*

$$u_1^0(x) = u_1^-(x) + x(1-x)\left\{\sin^2 30x + \sin 10x + 3\right\}/5,$$
$$u_2^0(x) = u_2^-(x) + x(1-x)\left\{\sin^2 20x + \sin 40x + 3\right\}/10.$$

As in Experiment 1, $\mathbf{u}_0 \in [\mathbf{u}^-, \mathbf{u}^+]$. *The evolution of* u_1 *is depicted in Figure* 4.2; *again* u_2 *took a similar course. Again, these initial data seem to be attracted to* $\mathbf{u}^+$.

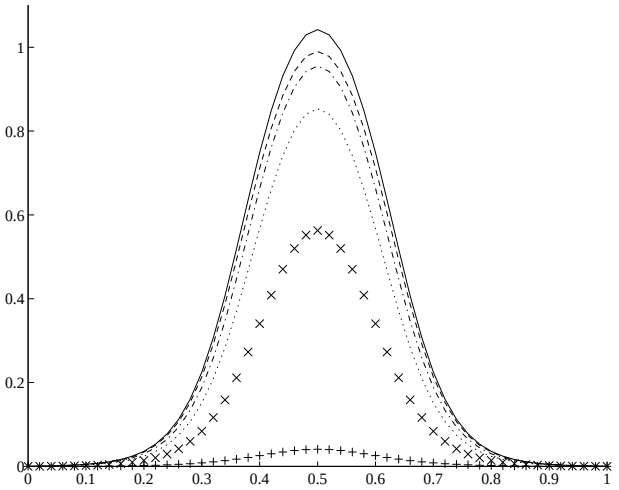

FIG. 4.3. *Results of Experiment* 3, u_1 *against* x, *with steady states* u_1^-, –; $t = 0$, - -; $t = 7.5$, -.; $t = 15$, ..; $t = 22.5$, ×; $t = 30$, +.

As far as the behavior of the system (3.1) below $\mathbf{u}^- = (u_1^-(x), u_2^-(x))$, $x \in (0,1)$, is concerned, we may proceed along the same lines by proving the following lemma.

LEMMA 4.3. *Under the assumptions of Theorem* 3.3, *case* 2(c), *the system*

$$\left\{ \begin{array}{rcl} d\,\tilde{w}_1''(x) - \tilde{w}_1(x) + (\alpha+\epsilon)\tilde{w}_2(x) & = & 0, \\ g(\tilde{w}_1(x)) - \beta\tilde{w}_2(x) & = & 0, \end{array} \right. \tag{4.3}$$

subject to homogeneous Dirichlet boundary conditions, admits two nontrivial classical solutions for a suitable choice of $\epsilon > 0$. *Both of them are upper solutions for problem* (3.1).

Suppose that $\tilde{\mathbf{u}} = (\tilde{u}_1(x), \tilde{u}_2(x))$, $x \in (0,1)$, is the smaller of these two solutions. Then by use of comparison theorems we have

$$\mathbf{0} \le \tilde{\mathbf{u}} \le \mathbf{u}^-,$$

and $[\mathbf{0}, \mathcal{U}(t)\tilde{\mathbf{u}}]$, $t > 0$, is a contracting rectangle about $\mathbf{0}$ in X.

We present a computer simulation for this case which supports our conjecture that $\mathbf{0}$ is GAS in the rectangle $[\mathbf{0}, \tilde{\mathbf{u}}]$ of the cone X_+.

EXPERIMENT 3. *We made the same parameter choices as in Experiment* 1. *We took initial data*

$$\begin{aligned} u_1^0(x) &= 19\,u_1^-(x)/20, \\ u_2^0(x) &= g(u_1^0(x)) \end{aligned}$$

so that $\mathbf{u}_0 \in [\mathbf{0}, \mathbf{u}^-]$. *The evolution of* u_1 *is depicted in Figure* 4.3; u_2 *followed a similar course and is not shown. It seems that this choice of initial data is attracted to* $\mathbf{0}$. *For this small value of* d, *we see a spatial localization effect; an epidemic starting with a peak below the "saddle point" solution* $\mathbf{u}^- = (u_1^-(x), u_2^-(x))$ *is not only extinguished but also "localized" in space.*

The case where initial data intersect the separatrix solution $\mathbf{u}^-$ is much more complex; we require global information on the separating manifold to determine the destiny of solutions.

Unfortunately we have been able to provide only partial answers by analytic methods; rigorous results concerning the domains of attraction of $\mathbf{0}$ and $\mathbf{u}^+$ will be dealt with in a subsequent paper.

5. Higher-dimension space domains. We now consider whether the results obtained in sections 3 and 4 apply when systems (1.2) and (1.3) are posed on multidimensional space domains Ω. In fact, we will mainly be concerned with just two simple examples, (i) where Ω is a two-dimensional disc and (ii) where Ω is a two-dimensional interval, e.g., $[0,1] \times [0,1]$. Most of our arguments will be based on numerical simulation.

For $\Omega \subset \mathbf{R}^n$ $(n \geq 2)$, [10] used a variational technique to prove, provided γ sufficiently large and d sufficiently small, that system (1.3) has at least one positive solution $\mathbf{u}^+$, which is a local minimum of the energy functional

$$E := \int_\Omega \left\{ \frac{1}{2} d |\nabla u_1|^2 + F_\gamma(u_1) \right\} d\mathbf{x}. \tag{5.1}$$

The mountain pass lemma was then applied (since $\mathbf{0}$ is always a local minimum of (5.1)) to deduce the existence of at least one more nontrivial solution of (1.3) ($\mathbf{u}^-$, say), which is a saddle point for the energy functional E. However, [10] does not provide upper bounds on the numbers of solutions to (1.3), unlike our Theorem 3.3 for the one-dimensional case. (Very few facts are known about the counting of solutions to nonlinear elliptic equations in general; see [9].) Further, note that system (1.2) is *not* a gradient system with energy E; therefore a saddle point for E is not necessarily a saddle point for the dynamics of (1.2), although this appears to be so in our case.

We conjecture that, *provided that our space domain is convex*, we may find a local minimum $\mathbf{u}^+$ and a saddle point $\mathbf{u}^-$ of E, of form similar to the $\mathbf{u}^-$, $\mathbf{u}^+$ found in section 3, such that $\mathbf{0}$, $\mathbf{u}^-$, and $\mathbf{u}^+$ together control the dynamics of (1.2), in the same way as for the one-dimensional case shown in section 4.

Concerning the shape of steady-state solutions, we explored the case where Ω is a two-dimensional disc. We set the radius equal to $1/2$ (without loss of generality, since it may be absorbed in d by rescalings). If we restrict attention to axisymmetric solutions $u_1 = u_1(r)$, $u_2 = u_2(r)$ of (1.3), we then simply have to find regular u_1 satisfying the ODE

$$\frac{d}{r}\frac{d}{dr}\left(r \frac{du_1}{dr} \right) - u_1 + \gamma g(u_1), \tag{5.2}$$

supplemented by the conditions

$$u_1(1/2) = 0 \qquad \text{and} \qquad u_1'(0) = 0. \tag{5.3}$$

We have not performed an analytical study of this problem in the spirit of section 3; however, we have solved it numerically for a wide range of d and γ, using a shooting method. (N.B.: Care must be exercised in avoiding singularities at $r = 0$.) In fact, we have been unable to produce more than two positive solutions for any values of γ, d; it seems that an analogue of counting Theorem 3.3 may hold for axisymmetric steady states in this case, but we do not have a proof of this. (To construct a proof, we need to consider generic behavior of the new "time map" $t \mapsto u_1(1/2)$, where $u_1(1/2)$ is given by solving (5.2) as an initial value problem with data $u_1(0) = t$, $u_1'(0) = 0$.) Of course, we have not ruled out extra nonaxisymmetric steady-state solutions.

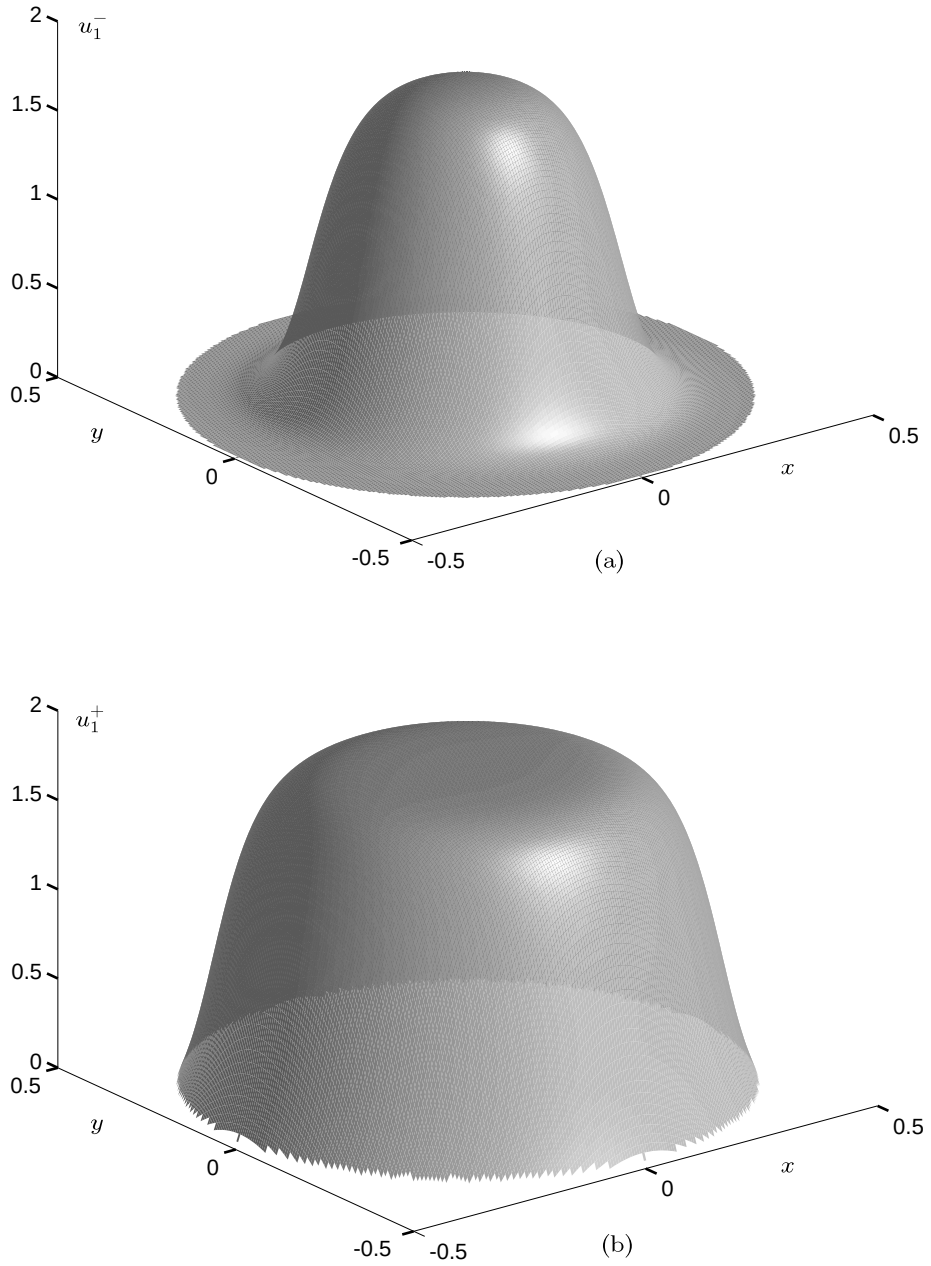

FIG. 5.1. *Axisymmetric steady-state solutions on a two-dimensional disc, radius* 1/2, *with* $\gamma = 2.35 > \gamma_{crit}$, $d = 0.001 < d_{crit}(\gamma)$; (a) u_1^-, (b) u_1^+.

For $\gamma = 2.35$ and $d = 0.001$, there are exactly two nontrivial solutions $u_1^- < u_1^+$ to problem (5.2), (5.3) (in effect like Theorem 3.3, case 2(c)). We have plotted these against (x, y) in Figure 5.1. The shapes are like those from the one-dimensional case depicted in Figure 3.3; in particular, u_- is bell shaped. (The bell may be made narrower by reducing d.)

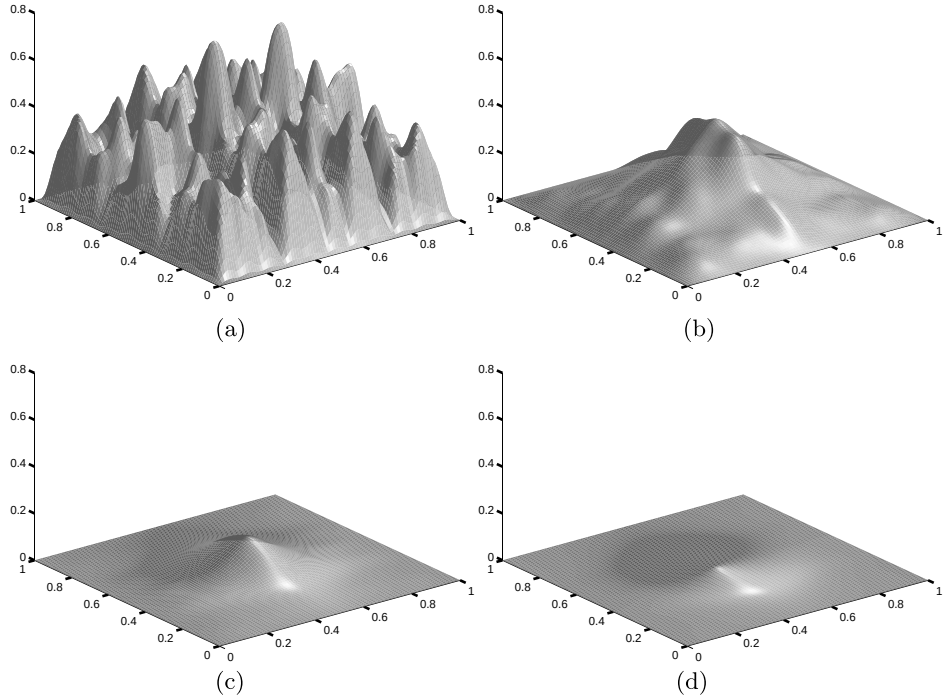

FIG. 5.2. *Results of Experiment* 4*, with bacterial concentration* u_1 *plotted against* x*,* y *for* (a) $t = 0$*,* (b) $t = 4.0$*,* (c) $t = 8.0$*, and* (d) $t = 12.0$*. The localization of the epidemic as it is extinguished is clear.*

We now move on to consider the dynamical part of our conjecture; we consider some numerical simulation of (1.2) posed on the unit square space domain $[0,1]\times[0,1]$. We did not consider a steady-state analysis of this problem above, because it is not possible to convert it to an ODE to which our shooting method code may be applied. However, as we show below, it is possible to detect stable steady states by starting with suitable initial data and letting the code run for a sufficiently long time. However, as an added bonus, the simulation in Experiment 5 seems able to detect the presence of a saddle point.

EXPERIMENT 4. *We took* $g(u) = u^2/(1+u^2)$*,* $\alpha = 2.5$*,* $\beta = 1.0$ (*so that* $\gamma = 2.5$)*, and* $d = 0.001$ *and solved* (1.2) *under homogeneous Dirichlet conditions at the boundary of the space domain* $[0,1]\times[0,1]$*. We simulated* (1.2) *by means of an alternating direction implicit scheme* (*see* [13])*, coupled with a backward Euler code to solve the ODE for* u_2*.* (*This technique is numerically very stable.*) *We took initial data*

$$u_1^0(x,y) = 0.3\sin\pi x\sin\pi y + n(x,y),$$
$$u_2^0(x,y) = g(u_1^0(y,x)),$$

where $n(x,y) > 0$ *is the "noisy" function defined by*

$$n(x,y) := \frac{1}{4}\sin^2 5\pi x\sin^2 4\pi y + \frac{1}{4}\sin^2 3\pi x\sin^2 7\pi y + \frac{1}{10}\sin^2 9\pi x\sin^2 11\pi y. \tag{5.4}$$

The evolution of bacterial concentration u_1 *is shown in Figure* 5.2. (*The evolution of the concentration of infective humans followed a similar course and is not shown.*)

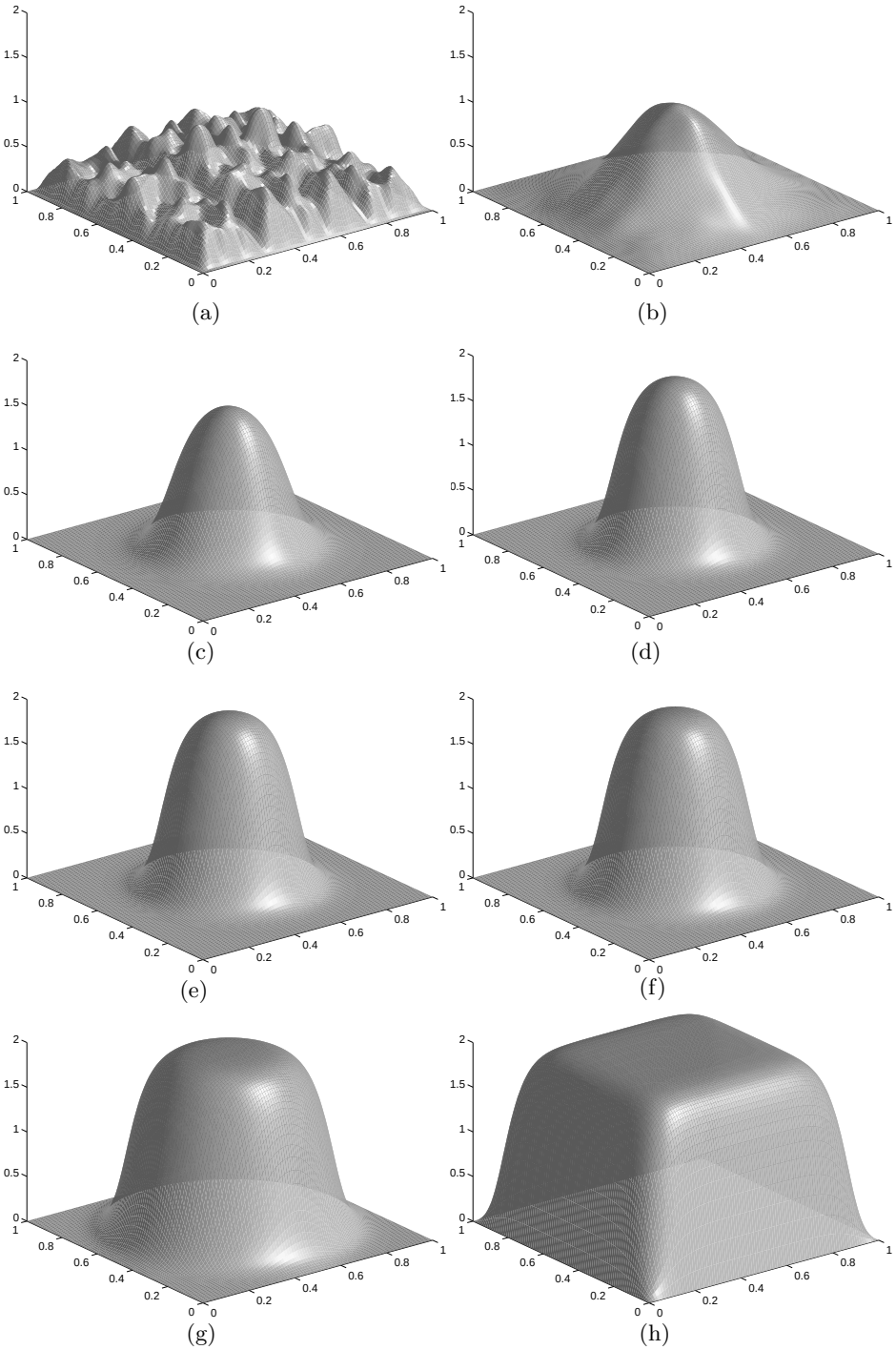

FIG. 5.3. *Results of Experiment* 5, *with bacterial concentration* u_1 *plotted against* x, y *for* (a) $t = 0$, (b) $t = 5$, (c) $t = 10$, (d) $t = 15$, (e) $t = 20$, (f) $t = 25$, (g) $t = 50$, *and* (h) $t = 250$. $\mathbf{u}$ *increases rapidly to what appears to be the neighborhood of a saddle point solution. Only on a much longer time scale does* $\mathbf{u}$ *evolve to the stable endemic state.*

This choice of initial data is attracted to $\mathbf{0}$*, and the localization of the epidemic as it is extinguished is clear, just as in Figure* 4.3 *for the one-dimensional case.*

EXPERIMENT 5. *Our conditions and method were exactly those of Experiment* 4*, except that we took the larger initial data*

$$u_1^0(x,y) = 0.5 \sin \pi x \sin \pi y + n(x,y),$$
$$u_2^0(x,y) = g(u_1^0(y,x)),$$

where the choice of the "noisy" function $n(x,y)$ *was as before. The evolution of bacterial concentration* u_1 *is shown in Figure* 5.3*; the solution is quickly attracted up to a symmetric bell-like shape which enlarges very slowly. Only on a much longer time scale does the solution approach what appears to be a final stable steady state* $\mathbf{u}^+$*. It would seem that the bell-shaped profile appearing in Figure* 5.3(e) *is close to some saddle state* $\mathbf{u}^-$*. The solution is quickly attracted to the stable manifold of this steady state and to the neighborhood of the steady state itself. Presumably it lingers there for so long, because the unstable eigenvalue has small magnitude. This explanation is (of course) a conjecture.*

We have not been able to find initial data which give behavior qualitatively different from that of Experiments 5 and 6. This is good evidence that even when the space domain Ω is multidimensional, *provided that it is convex*, the infinite-dimensional system (1.2) inherits basically the same structure as the underlying finite-dimensional ODE system (1.1) (i.e., bistable behavior with a saddle point).

The case where Ω is nonconvex is more complicated. For example, [12] showed that when Neumann boundary conditions are applied to a domain with a narrow "neck," extra *stable* steady-state solutions of scalar reaction diffusion equations must exist (if parameters are chosen appropriately). In a forthcoming paper, we will consider the dynamics of (1.2) on such domains, with homogeneous Dirichlet boundary conditions in force.

REFERENCES

[1] V. I. ARNOLD, *Ordinary Differential Equations*, MIT Press, Cambridge, MA, 1973.

[2] V. CAPASSO, *Mathematical Structures of Epidemic Systems*, Lecture Notes in Biomath. 97, Springer-Verlag, Heidelberg, 1993.

[3] V. CAPASSO AND K. KUNISCH, *A reaction-diffusion system arising in modelling man-environment diseases*, Quart. Appl. Math., 46 (1988), pp. 431–450.

[4] V. CAPASSO AND L. MADDALENA, *Convergence to equilibrium states for a reaction-diffusion system modelling the spatial spread of a class of bacterial and viral diseases*, J. Math. Biol., 13 (1981), pp. 173–184.

[5] V. CAPASSO AND L. MADDALENA, *Saddle point behaviour for a reaction-diffusion system: Application to a class of epidemic models.* Math. Comput. Simulation, 24 (1982), pp. 540–547.

[6] V. CAPASSO AND S. L. PAVERI-FONTANA, *A mathematical model for the* 1973 *cholera epidemic in the European Mediterranean region*, Revue d'Epidemiologie et de Santé Publique, 27 (1979), pp. 121–132.

[7] J. K. HALE, *Ordinary Differential Equations*, Wiley-Interscience, New York, 1969.

[8] D. W. JORDAN AND P. SMITH, *Nonlinear Ordinary Differential Equations*, 2nd ed., Clarendon Press, Oxford, UK, 1987.

[9] P. L. LIONS, *On the existence of positive solutions of semilinear elliptic equations*, SIAM Rev., 24 (1982) pp. 441–467.

[10] E. MIRENGHI, *Equilibrium solutions of a semilinear reaction-diffusion system*, Nonlinear Anal., 11 (1987), pp. 393–405.

[11] I. NÅSELL AND W. M. HIRSCH, *The transmission dynamics of schistosomiasis*, Comm. Pure Appl. Math., 26 (1973), pp. 395–453.

[12] H. Matano, *Asymptotic behaviour and stability of solutions of semilinear diffusion equations*, Publ. Res. Inst. Math. Sci., 15 (1979), pp. 401-454.
[13] K. W. Morton and D. F. Mayers, *Numerical Solution of Partial Differential Equations*, Cambridge University Press, Cambridge, UK, 1994.
[14] *Proceedings of the International Seminar on Diffusion and Treatment of Cholera Infection*, National Institute of Health of Italy, ISS, Rome, 1974.
[15] J. Smoller, *Shock-Waves and Reaction Diffusion Systems*, Springer-Verlag, New York, 1983.
[16] J. Smoller and A. Wasserman, *Global bifurcation of steady state solutions*, J. Differential Equations, 39 (1981), pp. 269–290.
[17] R. E. Wilson, *An Analysis of Two Problems from Applied Mathematics*, D. Phil. thesis, University of Oxford, 1995.